Experimental Investigation of an Argon Hollow Cathode

R. P. Stillwell*
The BDM Corporation, McLean, Virginia
and
R. S. Robinson,† H. R. Kaufman,‡ and R. K. Cupp§
Colorado State University, Fort Collins, Colorado

An argon hollow cathode was investigated. It was found that the condition of the insert and tip material had a direct effect on discharge power. Temperature profiles of the tip, cathode tube, and anode were taken. Thermal losses were calculated from the temperature profiles. As emission increased, the measured thermal losses constituted a smaller fraction of the total discharge power. At the higher emission levels, a higher fraction of the discharge power went to gas collisional effects and wall losses outside the cathode region. Temperature profiles of the insert were measured. It was found that the majority of emission occurred in the 6 mm of insert closest to the tip.

Introduction

HOLLOW cathodes are a critical component of inert-gas ion thrusters. As such, understanding their operation is important.

The hollow cathode investigated employed oxide-free components and was mechanically assembled (no welding). This approach has advantages from the research viewpoint in that fabrication of such cathodes is straightforward and the work functions of the surface are well known. Furthermore, the assembled construction should avoid the thermal stress problems of welded assembly using dissimilar materials and section thickness.

In earlier work,[1] a rolled Ta foil insert was found to be an efficient oxide-free emission surface. This present investigation continues the study of a rolled Ta foil insert. Graphite tips were also used in the previous study.[1] The work reported herein describes operation with both graphite and tungsten tips.

Apparatus and Procedure

The typical test arrangement for a hollow cathode is indicated in Fig. 1. The body of the hollow cathode was a 6.4-mm outside-diameter Ta tube, 6.3 cm long. The tube thickness was 0.51 mm, unless otherwise indicated. The Ta tube was mounted in an Al block, onto which the other components were connected. The rolled-foil inserts used in the test were fabricated from 0.013-mm-thick Ta. The inserts were typically 4×8.6 cm, textured by pressing the foil against 50-grit abrasive paper, using an elastomer for pressure. The inserts were then rolled into an approximately five-turn insert with a length of 4 cm. Where noted, the length was varied and untextured foil was used.

A stainless steel perforated cylinder, 5.8 cm in diameter and 10.2 cm long, was used as the anode. The position of the anode in Fig. 1 is displaced for clarity. The tip of the cathode was flush with the near end of the anode during these tests.

The only gas introducted into the 45-cm-diameter vacuum chamber was the Ar flow through the hollow cathode.

An internal starting electrode described previously[1] was used throughout this investigation. After initiation, the starting discharge was turned off. Because there was no external source of heat after the starting discharge was turned off, a minimum emission was required to maintain operation. This minimum depended on Ar flow and cathode geometry, but was typically 3-4 A equiv (A equiv related to mass flow rate by mass flow × Avogadro's number × electronic charge × atomic weight).

Unless otherwise specified, the tip was a 6.4-mm diameter disk, 1 mm thick, with a centered 1.0-mm-diameter hole. Because this design is a simple disk without provision for centering in the Ta tube, a 0.013-mm-thick piece of Ta was spot welded to the Ta tube to perform this centering function.

The testing procedure included taking current-voltage characteristics, with the current varied from the minimum required to maintain operation up to either the power supply limit (25 A) or the emission limit.[2] Tests designed to determine thermal power losses involved temperature measurements. These temperature measurements were taken with thermocouples or an optical pyrometer, depending on the temperature range. Tests were typically conducted at Ar flows of 0.6, 0.7, 0.8, 0.9, and 1.0 A equiv.

The use of the optical pyrometer in the temperature measurements required corrections to be made to the pyrometer readings. The corrections were for emissivity (nonblackbody) and the absorption by the vacuum facility glass. The correction for the emissivity is given by[3]

$$\frac{1}{T_{t,l}} = \frac{1}{T_{\text{obs},l}} + \frac{\lambda \ell n \epsilon_\lambda}{c} \tag{1}$$

where $T_{t,l}$ is the true temperature, $T_{\text{obs},l}$ is the observed temperature, λ is the wavelength of the filter in the pyrometer (0.653μ), ϵ_λ is the spectral emissivity of the material, and c is the natural constant ($1.43 \times 10^4 \mu k$).

Temperature measurements were made with three materials, graphite, W, and Ta. Their spectral emissivities at a wavelength of 0.653 μ are $\epsilon_{\lambda,\text{graphite}} = 0.745 - 1.88 \times 10^{-5}\, T$ (Ref. 4), $\epsilon_{\lambda,w} = 0.4757 - 2.095 \times 10^{-5} T$ (Ref. 5), and $\epsilon_{\lambda,\text{Ta}} = 0.5353 - 5.655 \times 10^{-5} T$ (Ref. 6). It should be noted that the expression for the spectral emissivity of tantalum was a least-squares fit of experimental data.[6] The correlation coefficient of the fit was 0.734.

Presented as Paper 82-1890 at the AIAA/JSASS/DGLR 16th International Electric Propulsion Conference, New Orleans, La., Nov. 17-19, 1982; received Dec. 10, 1982; revision received Jan. 20, 1984.

*Staff Member. Member AIAA.
†Associate Professor, Department of Physics. Member AIAA.
‡Professor, Department of Physics. Associate Fellow AIAA.
§Research Assistant, Department of Physics.

The correction for the intensity absorption by the vacuum facility glass is given by[7]

$$\frac{1}{T_{t,2}} = \frac{1}{T_{\text{obs},2}} + A \tag{2}$$

where $T_{t,2}$ is the true temperature of a black body, $T_{\text{obs},2}$ is the observed temperature of a black body, and A is the correction for the glass absorption. The temperature of the facility wall should not change significantly during tests, so the value of A should be expected to be independent of the facility wall temperature.

Combining the two equations yields

$$\frac{1}{T_t} = \frac{1}{T_{\text{obs}}} + \frac{\lambda \ell n \epsilon_\lambda}{c} + A \tag{3}$$

The last equation incorporates both temperature corrections. The true temperature of the nonblack body material with the glass absorption correction is represented by T_t and T_{obs} is the observed temperature using the pyrometer.

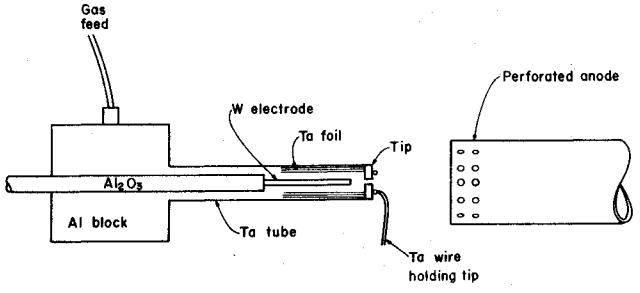

Fig. 1 Hollow cathode assembly.

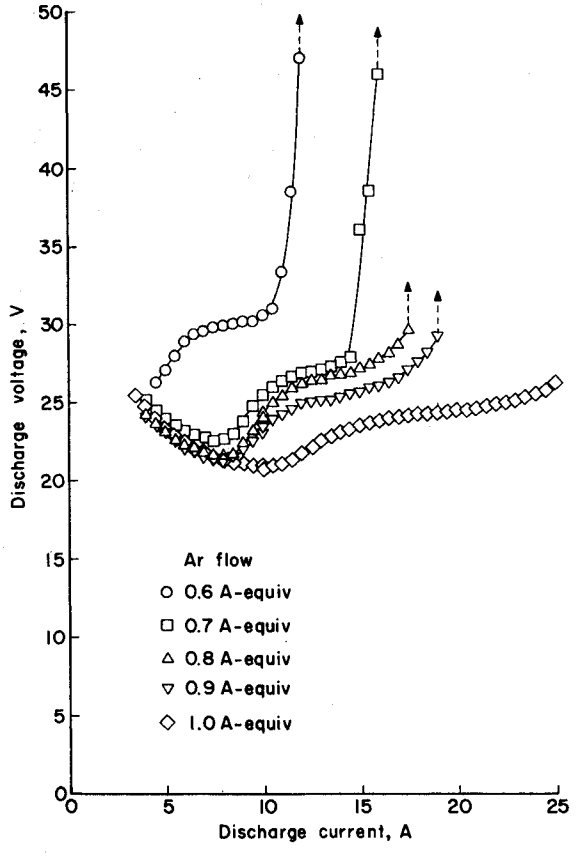

Fig. 2 Comparison of current-voltage characteristics for several values of Ar flow.

To determine the value of A, a thermocouple was spot welded to a Ta wire. The wire was heated and values of A were calculated from the last equation. The values of A were measured over the temperature range 1290 to 1959 K. An average value of $A = -3.70 \times 10^{-5} \pm 1.70 \times 10^{-5} \text{K}^{-1}$.

Effect of Argon Flow

Most tests were conducted for Ar flows of 0.6 to 1.0 A equiv. All tests had the characteristic that as the Ar flow was increased (all other parameters remaining constant), the power required for a given emission (discharge current) decreased and the emission limit increased. This is shown for data taken with a W tip in Fig. 2. The emission limits are indicated by dashed lines in the figure.

The general variation of emission limit with Ar flow rate has been observed previously many times. The exact magnitude of emission limits, however, also depends on the cathode geometry used.

Insert Length and Condition

After the cathode emission has been initiated by the starter electrode, the discharge power is the only heat input to the cathode. Much of the discharge power should appear as heating power inside the cathode. A change in insert configuration that reduces heat flow to the outside of the cathode should thus be expected to reduce the power required to maintain emission temperature at the inside of the insert, which, in turn, should reduce the discharge voltage required for a given emission level.

With this reasoning in mind, textured (described in the Apparatus and Procedure section) and untextured foil inserts both were compared in terms of operating characteristics. The intent of the texturing was to minimize contact between foil layers. At the high operating temperatures for the inside layers of the foil insert, some bonding would be expected to take place at any contact area. With plain surfaces, a high degree of direct thermal loss would be expected after this bonding takes place. With a textured surface, however, thermal conduction must follow a longer, labyrinthine path.

A comparison of cathode performance for textured and untextured inserts is shown in Fig. 3. Comparisons were made

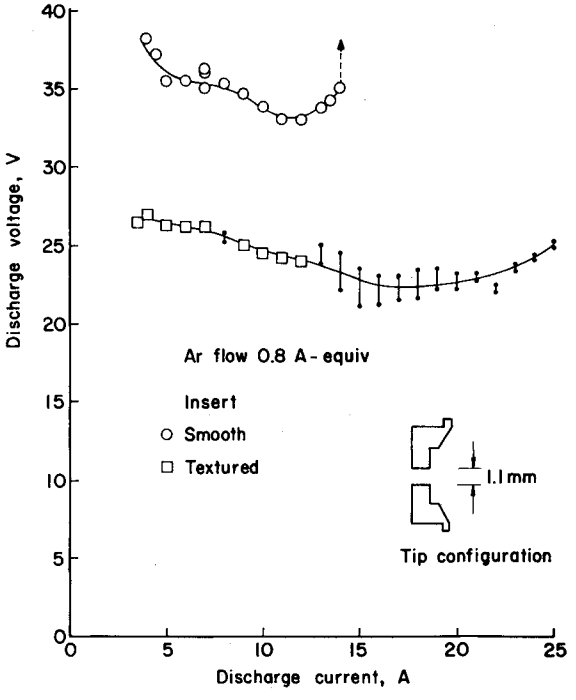

Fig. 3 Comparison of discharge current-voltage characteristics for textured and untextured inserts.

for several Ar flows, and in all cases the textured insert showed substantial (10-40%) reduction in discharge power. It should be noted that in these comparisons a graphite tip was used. The tip configuration is also shown in Fig. 3.

The textured inserts used in these tests apparently caused some oscillation (see vertical bar in Fig. 3 for range of the oscillations). Because these oscillations were sufficiently slow to be followed by visual observations of meters, they are assumed to be thermal/mechanical in origin, rather than associated only with plasma processes.

The insert length (axial) was also varied. One might expect a shorter insert to provide less electron emission, hence, to be less efficient. On the other hand, experience with oxide coated inserts indicates that most of the emission is from the first 2 mm near the tip, for Hg propellant.[8] Three insert lengths were tested, 1, 2.5, and 4 cm. These tests employed a W tip and were conducted at Ar flow rates of 0.6, 0.7, 0.8, 0.9, and 1.0 A equiv. The results were all similar; a typical test is shown in Fig. 4.

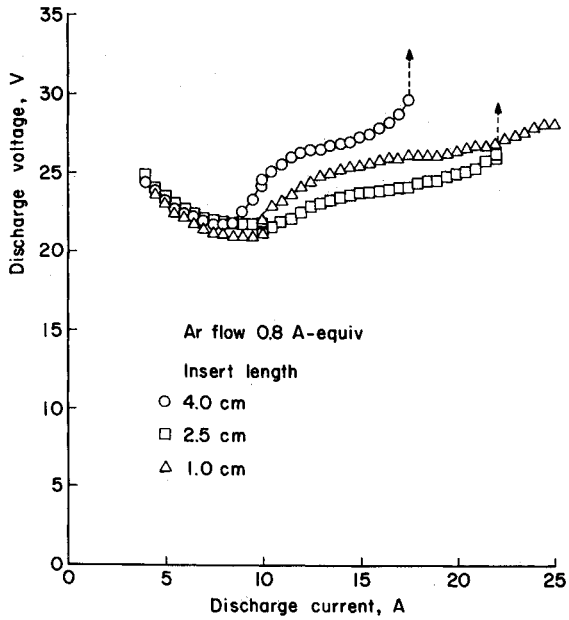

Fig. 4 Comparison of cathode performance for differenct insert lengths.

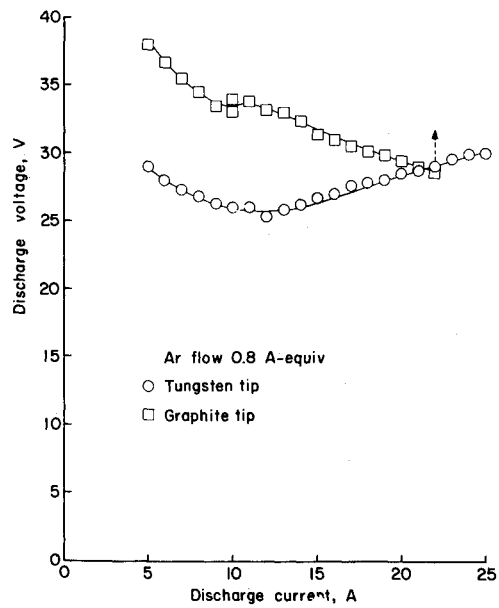

Fig. 5 Comparison of cathode performance for two different tip materials.

The tests of different insert lengths did not show a clearcut difference in voltage at a given emission, hence a difference in heating power. Where differences were found, the medium length (2.5 cm) showed the lowest discharge voltage. For maximum emission, the highest value was found for the shortest insert. Depending on the parameter of interest, then, somewhere in the 1 to 2.5 cm range of length appeared of most interest.

Tip Material

Two tip materials were tested, tungsten and high-density graphite. The cathode performance obtained using the two tip materials is indicated in Fig. 5. At all combinations of emission and Ar flow that could be compared, the W tip showed lower discharge powers than the graphite tip. In addition, the maximum emission was increased by the use of W.

The difference in power required for two tip materials is consistent with the hypothesis that the plasma discharge supplies whatever power is required for the emission surface to reach emission temperature.[1] Because the potential variation is small from the anode to the plasma within the hollow cathode, much of the discharge power appears as cathode heat.[9] Because the plasma is densest near the cathode tip, much of this heat is lost to the tip. While the tip itself is not believed to be a source of significant emission, its heat balance will directly affect the inside temperature of the foil insert, which is believed to be the major emission source.

Tip temperature profiles were taken at several Ar flows (0.6, to 1.0 A equiv). The temperatures were measured with an optical pyrometer. Figure 6 shows the difference in temperature for the two tip materials at various emission levels. For all Ar flows tested, it was found that the graphite tip had higher temperatures at all emission levels than the W tip. The tip temperatures also appear to be essentially independent of flow rates.

From the tip temperature profiles, it was possible to compute the power radiated from the tips. For these calculations, the total emissivities of graphite and tungsten

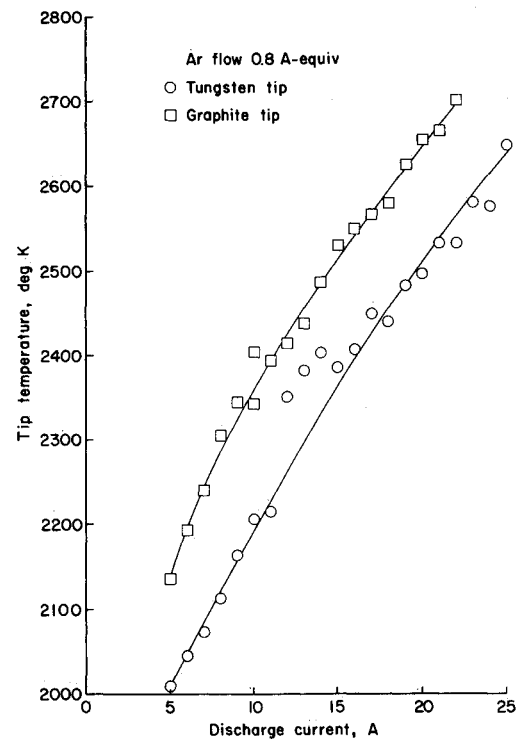

Fig. 6 Temperature of W and graphite tips for different emission levels.

were needed. For the tungsten, the total emissivity was founded by a linear least-squares fit to data, which yielded[10]

$$\epsilon_W = 0.0651 + 9.495 \times 10^{-5} T \quad (4)$$

where T is in K($\epsilon_W \sim 0.25$ to 0.32 for temperature range of interest). The value of total emissivity used for the graphite was 0.90. This value was chosen because high-density graphite (grade used HPD-1) typically had a total emissivity between 0.88 and 0.92.

The power radiated is given by

$$\text{Power radiated} = \epsilon A_{\text{Tip}} \sigma T^4 \quad (5)$$

where ϵ is the total emissivity, A_{Tip} is the surface area of one face of the tip (6.35 mm diameter), and σ is the Stefan-Boltzmann constant (5.67×10^{-8} watts $m^{-2}K^{-4}$). With the radiated power from the different tips calculated, the difference in radiated tip power was compared to the difference in discharge power. For the five Ar flow rates tested, it was found that the radiated tip power difference accounted for roughtly 44% of the discharge power difference of the two tip materials. This indicates that the tip material does directly affect the heat balance between the foil insert and the tip. It further implies that the difference is primarily due to the difference in radiation characteristics.

Temperature Profiles

With the purpose of evaluating thermal power losses more completely, temperature profiles of some of the other cathode components were taken during cathode operation using a W tip.

The temperature of the anode was measured with a thermocouple. It was found that the anode temperature varied from 530 to 670 K during cathode operation. A profile of the temperature gradient along the cathode tube was taken. The temperature along the first 20 mm of the Ta tube was measured using an optical pyrometer. To insure that the measurements were taken at the same position for the different emission levels, an Al alignment grating with slots every 2.54 mm was placed parallel to the cathode axis approximately 0.5 cm from the tube. Two thermocouples were spot welded to the cathode tube at positions 41.0 and 45.5 mm downstream of the tip. The temperature profile of the cathode tube, along with tip and anode temperature, are shown in Fig. 7 for three emission levels.

Firuge 7 shows that the temperature is highest at the tip and decreases downstream along the Ta tube. The temperature profile measured along the first 20 mm of the tube is linear with position (the origin defined as the edge of the tube in contact with tip). Measurements taken using a graphite tip indicated that the tube temperature is essentially independent of tip material.

Thermal Power Losses

Thermal power losses were calculated to determine if an accounting could be made of the majority of the discharge power. The power radiated from the tip has already been discussed previously (Tip Material section). The radiated power from the tip accounted for less than 5% of the total discharge power. The radiated power loss from the cathode tube was calculated by integrating the temperature profile along the tube, that is,

$$\text{Radiated tube power} = \int \epsilon_{\text{Ta}} T^4 \sigma \mathrm{d}A_{TS} = \sigma \pi d \int \epsilon_{\text{Ta}} T^4 \mathrm{d}\ell \quad (6)$$

where d is the outside diameter of the tube (6.4 mm), and ℓ is the position along the cathode tube axis. The expression used for the total emissivity of Ta,

$$\epsilon_{\text{Ta}} = -4.48 \times 10^{-3} + 1.182 \times 10^{-4} T \quad (7)$$

was found by a linear least-squares fit to published data.[11] The temperature profiles used was a linear fit to the data in the first 20 mm of the tube. It was felt that because of the linearity of the data that extrapolating the profile would give reasonable results. The total radiated power from the cathode tube can be divided into three regions, $\ell = 0$ to 2.03 mm, $\ell = 20.3$ to 17.18 mm, and $\ell = 17.18$ to 50.5 mm (50.5 mm is where the cathode tube enters the Al block). The central region, $\ell =$ 2.03 to 17.18 mm, is the region in which the data were obtained. The radiated power over this area comprises

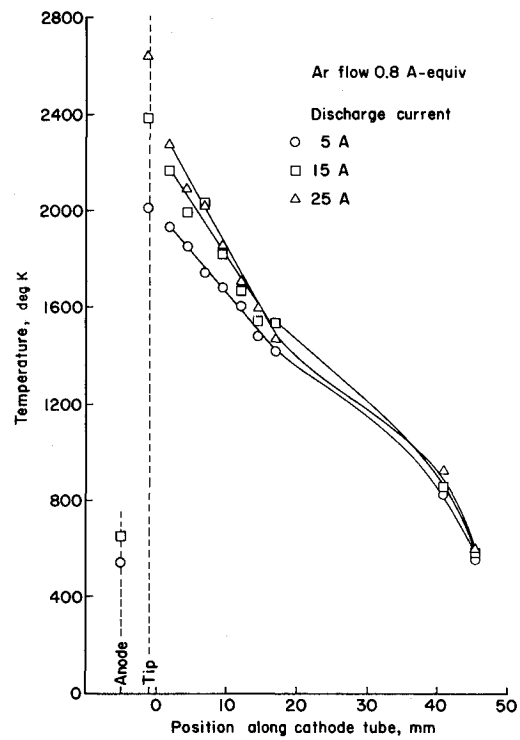

Fig. 7 Temperature profile of cathode components for three emission levels.

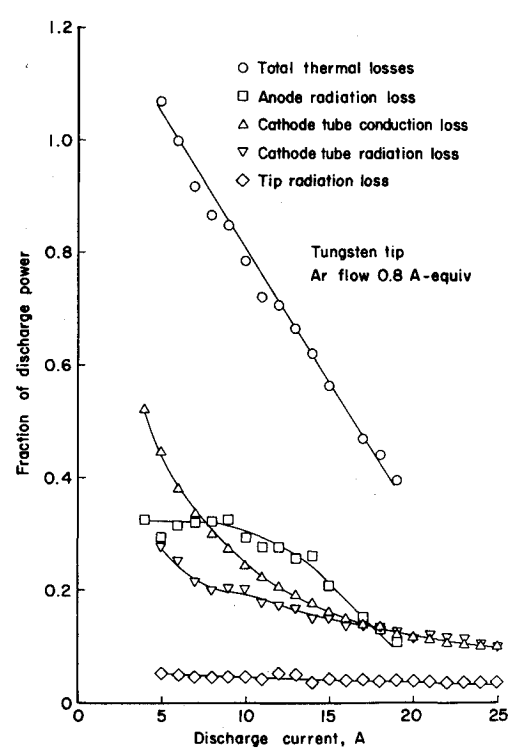

Fig. 8 Thermal power losses of cathode components.

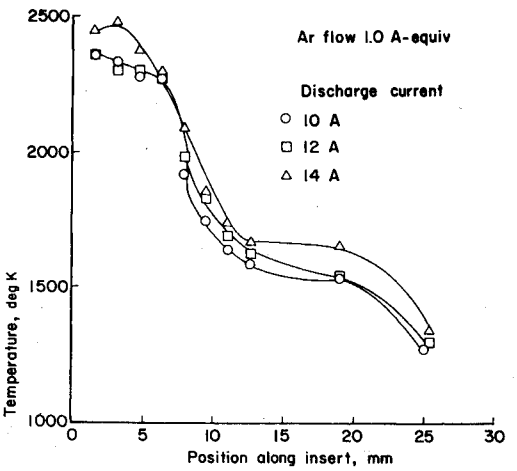

Fig. 9 Temperature profile of insert.

approximately 60% of the total radiated power of the cathode tube. The region closest to the tip, $\ell = 0$ to 2.03 mm, comprises approximately 20-25% of the power loss. There is probably little error in extending the temperature profiles through this region, since the profile is very linear and is extrapolated over only a short length. The third region, $\ell = 17.18$ to 50.5 mm, probably contains the most error, since the temperature profile is extended over a region twice the length over which the temperature profile was measured. However, since the temperature drops linearly and the radiated power is proportional to T^4, most of the radiated power would be concentrated in the length of the tube immediately adjacent to the measured region. This region contributes approximately 15-25% of the total power radiated from the cathode tube. The radiated power from the Ta tube is thus felt to be determined within perhaps ~20%. The power radiated from the tube accounts for 28 to 10% of the total discharge power, decreasing with increasing emission. The uncertainty in radiated power from the Ta should thus be a small part of the total power loss.

The two temperature measurements taken downstream of the tip at positions 4.10 and 4.55 cm were used to calculate conduction losses down the Ta tube. These measurements were taken downstream of the insert to avoid heat sources associated with internal emission.

The power loss due to conduction is given by

$$\dot{Q} = -kA_{TC}\frac{dT}{d\ell} \tag{8}$$

where k is the thermal conductivity and A_{TC} is the cross-sectional area of the cathode tube (0.195 cm^2). In calculating the conduction loss an average value of thermal conductivity of 0.59 W cm^{-1}K^{-1} was used.[12] The conduction power loss varied from 65 to 85 watts, increasing with emission level. This accounted for 50 to 10% of the discharge power, decreasing with emission level.

The anode radiation power loss is given by

$$\text{Radiated anode power} = \epsilon_{S.S}\sigma A_A (A^4 - 300^A) \tag{9}$$

where A_A is the surface area of the anode and $\epsilon_{S.S.}$ is the total emissivity of stainless steel. A value of $\epsilon_{S.S} = 0.5$ was used; this is for a piece of stainless steel heated and cooled repeatedly,[13] which is believed consistent with the observed discolored appearance. The anode area contribution to radiation (176.5 cm^2) was found by approximating the view factor for the interior surface of the anode. The anode radiated power varied from 36 to 100 watts, accounting for 33 to 11% of the total discharge power, decreasing with increasing emission level.

Figure 8 shows these thermal power losses both as a fraction of discharge power and a function of emission level. From the figure, it is seen that conduction of heat down the cathode tube, radiation from the cathode tube, and radiation from the anode contribute roughly equally to the thermal loss. As such, these loss mechanisms are of most interest.

It should be noted from Fig. 8 that the total thermal losses are 107% of the discharge power at an emission level of 5 A. This value is an indication of the error caused by the various approximations assumed in calculating the power losses. The thermal losses at low emission levels thus account for almost all of the discharge power.

Figure 8 also shows that as the emission level increases, more of the discharge power is unaccounted for. As the emission level increases, the glow near the tip orifice also increases. This glow is an indication of discharge power being lost directly through increased radiation from atoms and ions. One would also expect an increase in energy transport to the vacuum facility walls with energetic species to accompany an increase of observed glow.

Insert Emission

Hollow cathode emission is believe to be by field-enhanced thermonic emission.[14,15] With thermonic emission as an emission process, temperature profiles of the insert are of interest.

To measure the temperature of the insert, ten holes, each 1 mm in diameter, were drilled through the Ta tube and four outer layers of the textured insert over a distance of 25 mm. A fifth untextured turn was inserted within the outer four layers, pressed against the textured turns after the holes had been drilled. In this way the temperature of the innermost turn was measured with an optical pyrometer. The Ar flow was 1.0 A equiv, although only qualitative results could be found since there was gas leakage through the holes. The results of these measurements are shown in Fig. 9 for three emission levels.

Figure 9 shows that there is a substantial temperature drop at about 6 mm, indicating that most of the emission occurs from the first 6 mm of the insert. This is in agreement with the observations of Siegfried and Wilbur[8] in that the majority of emission occurs from a small portion of the insert closest to the tip. While they found that the emission occurred from the first 2 mm of the insert, their model[15] predicts that the portion of the insert contributing the majority of emission depends on the various cross sections of the propellant gas. Thus, since Hg was used, one would expect the insert length contributing to emission for an Ar hollow cathode to differ from that of an Hg hollow cathode.

Figure 9 also shows that, as the emission level is increased, the insert temperature at all positions increases. This increase with emission, however, is small.

Concluding Remarks

The investigation showed that a textured insert can reduce the discharge power and increase the maximum emission for an *Ar* hollow cathode. It also showed that the length of the insert is not an important parameter in the performance, as long as the insert is at least 1 cm in length. Tip material also proved to be an important consideration. The W tip exhibited better cathode performance and higher maximum emissions than graphite tips. This effect was due not only to higher power radiation from the graphite tip, but also to an internal heat balance with the insert.

The thermal losses for the entire cathode were calculated. This calculation indicated that, as emission increases, plasma collisions external to the cathode and vacuum facility wall losses constitute a greater fraction of the discharge power.

Insert temperature profiles were measured, indicating that the majority of emission occurs in the first 6 mm of the insert.

References

[1]Kaufman, H. R., Robinson, R. S., and Trock, D. C., "Inert Gas Thruster Technology," *Journal of Spacecraft and Rockets* Vol. 20, 1983, pp. 77-83.

[2]Kaufman, J. R. and Robinson, R. S., "Inert Gas Thrusters," NASA Contract Report CR-159813, Nov. 1979.

[3]Kostkowski, H. J. and Lee, R. D., "Theory and Method of Optical Pyrometry," NBS Monograph 41, in *Precision Measurements and Calibration,* Vol. 2, NBS SP-300, 1968, pp. 361-390.

[4]Thorn, R. J. and Simpson, O. C., "Spectral Emissivities of Graphite and Carbon," *Journal of Applied Physics* Vol. 24, 1953, p. 633.

[5]Larrabee, R. D., "Spectral Emissivity of Tungsten," *Journal of the Optical Society of America,* Vol. 49, 1959, p. 619.

[6]Parker, W. J. and Abbott, G. L., "Theoretical and Experimental Studies of the Total Emittance of Metals," in *Symposium on Thermal Radiation of Solids,* NASA SP-55, 1965, pp. 11-28.

[7]Foote, P. D., Fairchild, C. O., and Harrison, T. R., "Pyrometric Practices," NBS Technological Paper No. 170, 1921.

[8]Siegfried, D. and Wilbur, P. J., "Studies on Experimental Quartz Tube Hollow Cathode," AIAA Paper 70-2056, Oct. 1979.

[9]Siegfried, D., "Mercury Hollow Cathode Studies," in NASA Contract Report CR--135317, P. J. Wilbur, ed., Dec. 1977, pp. 69-95.

[10]King, W.J., "Emissivity and Absorption," *CRC Handbook of Chemistry and Physics,* 56th ed., CRC Press, Cleveland, Ohio, 1975, pp. E229-E230.

[11]Taylor, R. E., Davis, F. E., Powell, R. W., and Kimbrough, W. D., "Determination of Thermal and Electrical Conductivity, Emittance and Thomson Coefficient at High Temperatures by Direct Heating Methods," AFML-TR-69-277, Oct. 1969.

[12]Ho, C. Y., Powell, R. W., and Liley, P. E., "Thermal Conductivity of Selected Materials - Part 2," NSRDS-NBS 16, Feb. 1968.

[13]Sparrow, E. M. and Cess, R. D., *Radiation Heat Transfer,* McGraw-Hill, New York, 1978.

[14]Siegfried, D. and Wilbur, P. J., "An Investigation of Mercury Hollow Cathode Phenomena," AIAA Paper 78-705, April 1978.

[15]Siegfried, D. and Wilbur, P. J., "A Model for Mercury Orificed Hollow Cathodes: Theory and Experiment," AIAA Paper 82-1889, Nov. 1982.